

Supporting Information

Adaptability of the metal(III,IV) 1,2,3-trioxobenzene rod-like Secondary Building Unit for the production of chemically stable and catalytically active MOFs

Georges Mouchaham,^a Brian Abeykoon,^b Mónica Giménez-Marqués,^{a,c} Sergio Navalon,^c
Andrea Santiago-Portillo,^c Maame Affram,^a Nathalie Guillou,^a Charlotte Martineau,^a
Hermenegildo Garcia,^c Alexandra Fateeva,^b Thomas Devic^{a,d*}

^aInstitut Lavoisier, UMR 8180 CNRS Université de Versailles Saint-Quentin-en-Yvelines, Université Paris-Saclay, 45 avenue des Etats-Unis, 78035 Versailles cedex, France ; ^b Université Claude Bernard Lyon 1, Laboratoire des Multimatériaux et Interfaces, UMR CNRS 5615, F-69622 Villeurbanne, France; ^c Instituto Universitario de Tecnología Química CSIC-UPV and Departamento de Química, Universidad Politécnica de Valencia, Av. De los Naranjos s/n, 46022 Valencia, Spain.; ^d Institut des Matériaux Jean Rouxel (IMN), Université de Nantes, CNRS, 2 rue de la Houssinière, BP 32229, 44322 Nantes cedex 3, France.

Table of content:

A.	Synthetic procedures	SI-2
B.	XRD analysis and structure determination	SI-3
C.	SEM and EDX	SI-8
D.	Solid State NMR	SI-9
E.	N ₂ sorption measurements	SI-12
F.	Thermal analysis	SI-12
G.	Solid state UV spectroscopy	SI-13
H.	Stability tests	SI-14
I.	EPR measurements	SI-15
J.	Raman experiments	SI-15
K.	Catalytic tests	SI-16

A. Synthetic procedures:

All chemicals were purchased from commercial sources and used without any further purification. 5,10,15,20-tetrakis(3,4,5-trihydroxyphenyl)porphyrin or H₁₄-PorphGal (phenolic and pyrolic protons accounting for 12 and 2 respectively) has been prepared following a previously reported procedure.^[1]

The direct preparation of metallated Co(II)-5,10,15,20-tetrakis(3,4,5-trihydroxyphenyl)porphyrin (Co-H₁₂-PorphGal) was also attempted, with no success yet. First, the reaction of H₁₄-PorphGal with Co(II) acetate in DMF leads to the formation of poorly defined insoluble solids arising from the coordination of the Co ion by the 1,2,3-trioxobenzene moieties. To circumvent this problem, the metalation was carried out on the protected version 5,10,15,20-tetrakis(3,4,5-trimethoxyphenyl)porphyrin (H₂Me₁₂-PorphGal). Nevertheless, the deprotection of the methoxy groups, which requires rather harsh conditions (BBr₃ in excess, see ^[1]) is accompanied by the demetalation of the porphyrinic core, leading finally to twice protonated H₁₆-PorphGal²⁺ ligand. Hence, attempts to directly prepare metallated MIL-173(Zr, RE)s were not carried out.

MIL-173(Zr): H₁₄-PorphGal (100 mg, 0.12 mmol) was combined with 5.6 mL of DMF and 3.2 mL of 1M HCl aqueous solution in a 40 mL glass vial. To the resultant mixture, 1.2 mL of a freshly prepared 0.133 M solution of ZrCl₄ (0.16 mmol) in 1 M aqueous HCl was added and then sonicated for 10 mins at room temperature. Afterwards, the suspension was heated at 130 °C for 23 hours, where the temperature was increased over 3 hours to reach the isotherm and then cooled down to room temperature over 3 hours. The solid was recovered by centrifugation, washed 3 times with DMF and 3 times with acetone to remove any unreacted starting material. After drying, the MOF was obtained as a dark violet solid in a 74% yield (90 mg). Elemental analysis: Calculated for {Zr₂(H₆-PorphGal)}·(DMA)₄(H₂O)₄, %C (50.63), %N(4.74); experimental, %C (50.56), %N(4.70).

Co-MIL-173(Zr): Dry MIL-173(Zr) (240 mg, 0.246 mmol) was combined with anhydrous Co(OAc)₂ (65.5mg, 0.370 mmol) in 20 mL of DMF and heated at 120 °C for 48 hours. The solid was recovered by centrifugation, washed 3 times with DMF, 3 times with deionized water and 3 times with acetone to remove any unreacted starting material. After drying, the MOF was obtained as a dark red solid in 83 % yield (210 mg). Elemental analysis: Calculated for {Zr₂(H₄-Co-PorphGal)}·(DMA)₂(H₂O)₁₇, %C (40.19), %N(5.86); experimental, %C (40.10), %N(5.81).

MIL-173(La): H₁₄-PorphGal (80 mg, 0.100 mmol) and LaCl₃.6H₂O (52.6 mg, 0.149 mmol) were combined with 2 mL of DMF and 2 mL of deionized water in a 12 mL glass vial and sonicated for 10 min at room temperature. The resultant suspension was then heated at 120 °C for 12 hours where the temperature was increased over 2 hours to reach the isotherm and then cooled down to room temperature over 4 hrs. The solid was recovered by centrifugation, washed 3 times with DMF and 3 times with anhydrous ethanol to remove any unreacted starting material. After drying, the MOF was obtained as a dark purple solid in a 59% yield (64 mg).

MIL-173(Ce): H₁₄-PorphGal (80 mg, 0.100 mmol) and CeCl₃.7H₂O (55.6 mg, 0.150 mmol) were combined with 2 mL of DMF and 2 mL of deionized water in a 12 mL glass vial and sonicated for 10 min at room temperature. The resultant suspension was then heated at 120 °C for 12 hours where the temperature was increased over 2 hours to reach the isotherm and then cooled down to room temperature over 4 hours. The solid was recovered by centrifugation, washed 3 times with DMF and 3 times with anhydrous ethanol to remove any unreacted starting material. After drying, the MOF was obtained as a dark purple solid in a 60% yield (65 mg).

MIL-173(Y): H₁₄-PorphGal (50 mg, 0.062 mmol) and YCl₃.6H₂O (56 mg, 0.185 mmol) was combined with 2.5 mL of DMF and 2.5 mL of deionized water in a Teflon autoclave at room temperature. The resultant suspension was then heated at 120 °C for 12 hours where the temperature was increased over 2 hours to reach the isotherm and then cooled down to room temperature over 4 hours. The solid was recovered by centrifugation, washed 3 times with DMF and 3 times with anhydrous ethanol to remove any unreacted starting material. After drying the MOF was obtained as a dark violet solid in a 65% yield (40 mg).

B. XRD analysis and structure determination

Routine XRPD patterns (as those shown in Figures 2, S3, S4) were measured on flat samples using either a Siemens D5000 Diffractometer working in the (θ-2θ) mode by using CuKα radiation (λ = 1.5418 Å) or a high-throughput Bruker D8 Advance diffractometer working on transmission mode and equipped with a focusing Göbel mirror producing CuKα radiation (λ = 1.5418 Å) and a LynxEye detector.

The high resolution XRPD data of MIL-173(Zr) were measured at room temperature on a Bruker D8 Advance diffractometer with a Debye-Scherrer geometry, in the 2θ range 4-90°.

The D8 system is equipped with a Ge(111) monochromator producing Cu K α 1 radiation ($\lambda = 1.540598 \text{ \AA}$) and a LynxEye detector. Extractions from the peak positions, pattern indexing, whole powder pattern decomposition, direct space strategy used to complete the structural model as well as difference Fourier calculations and Rietveld refinement were carried out with the TOPAS program.^[2] The LSI-indexing method converged unambiguously to a tetragonal unit cell with satisfactory figure of Merit ($M20 = 25$). Structural determination was then initialized with the EXPO package,^[3] using EXTRA for extracting integrated intensities and SIR97 for direct-methods structure solutions, as well as with TOPAS for charge flipping method. The direct space strategy was then used to localize the organic moiety treated as rigid body. Guest moieties were localized by alternating difference Fourier maps with simulated annealing and the atomic coordinates of the corresponding atoms were then fixed. At its final stage (Table S1 and Figure S1), the Rietveld refinement involved 1 Zr atomic coordinate, 1 thermal global factor and 1 scale factor. CCDC 1544198 contains the supplementary crystallographic data for MIL-173(Zr).

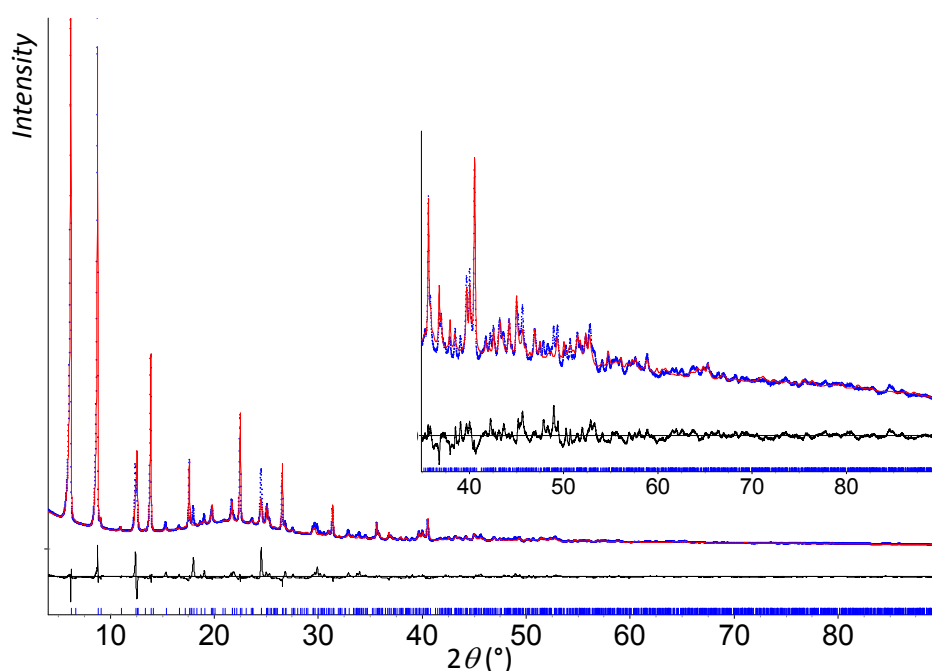


Figure S1. Final Rietveld plot of MIL-173(Zr) ($\lambda = 1.540598 \text{ \AA}$).

Table S1. Crystallographic data and Rietveld refinement parameter for MIL-173(Zr) :

Empirical formula	$C_{54} N_9 H_{55.4} O_{16.7}$
M_r	1280.17
Crystal system	Tetragonal
Space group	$I4_1/a m d$

a (Å)	28.4436(6)
c (Å)	14.9962(9)
V (Å ³)	12132.5(9)
Z	8
λ (Å)	1.5405981
Number of reflections	1316
No. of fitted structural parameters	3
R_p, R_{wp}	0.049, 0.076
R_{Bragg}, GoF	0.034, 10.4

Crystals of MIL-173(La) of sufficient size to be measured using a laboratory diffractometer were obtained. The chosen crystal (dimensions: 0.2 x 0.05 x 0.03 mm) was analysed at 293(2) K using a Geminini Oxford Diffractometer (MoK α radiation, $\lambda = 0.71069$ Å) equipped with a CCD camera and by using the related software.^[4] An absorption correction (analytical) has been applied.^[4] The structure was solved by direct methods using SHELXS-97 and refined with the full matrix least squares routine SHELXL-97.^[5] Non H-atoms were refined anisotropically, while N-H and C-H atoms were added as rigid bodies. Remaining phenolic hydrogen atoms (seem main text) were located on the Fourier map. The pore content was not refined and discarded using the SQUEEZE procedure.^[6] Crystallographic and refinements parameters are summarised in Table S2. CCDC 1544211 contains the supplementary crystallographic data for MIL-173(La).

MIL-173(La) and MIL-173(Zr) crystallize in different, but related tetragonal unit-cells ($a_{Zr} \sim \sqrt{2} * a_{La}, b_{Zr} \sim 2 * b_{La}$) leading to different asymmetric unit contents (1/4 and 1/8 of a H_nPorphGal respectively). Nevertheless, as shown in Figure S4c, they both present exactly the same framework (same SBU, same connection mode). The main difference can be seen along the inorganic chain (c) axis. While all the 1,2,3-trioxobenzene motifs are strictly aligned to this axis in MIL-173(La), they are slightly tilted in MIL-173(Zr) (Figure S4a-b).

Table S2. Crystallographic data and refinement parameters for MIL-173(La).

Empirical formula	La ₂ C ₄₄ H ₂₄ N ₄ O ₁₂
Formula weight	1078.5 g·mol ⁻¹
Temperature	293(2) K
Wavelength	0.71073 Å
Crystal system, space group	tetragonal, $I4/mmm$
Unit cell dimensions	$a = 20.6040(6)$ Å $c = 8.5110(6)$ Å
Volume (Å ³)	3613.1(3) Å ³
Z , calculated density	4, 0.991 g·cm ³

Adsorption coefficient	1.206 mm ⁻¹
F(000)	1052
Crystal size	0.02 x 0.05 x 0.03 mm
Theta range for data collection	2.589° - 29.400°
Limiting indices	-21 ≤ <i>h</i> ≤ 28, -25 ≤ <i>k</i> ≤ 27, -8 ≤ <i>l</i> ≤ 11
Reflections collected / unique	6428/1299 [R(int) = 0.0241]
Refinement method	full-matrix least squares
Data/Restraints/Parameters	1299/2/55
Goodness of fit on F ²	1.121
Final R indices [I > 2σ(I)]	R1 = 0.0371, wR2 = 0.0983
R indices (all data)	R1 = 0.0766, wR2 = 0.1004
Largest diff peak and hole (e·Å ⁻³)	0.593 and -0.729

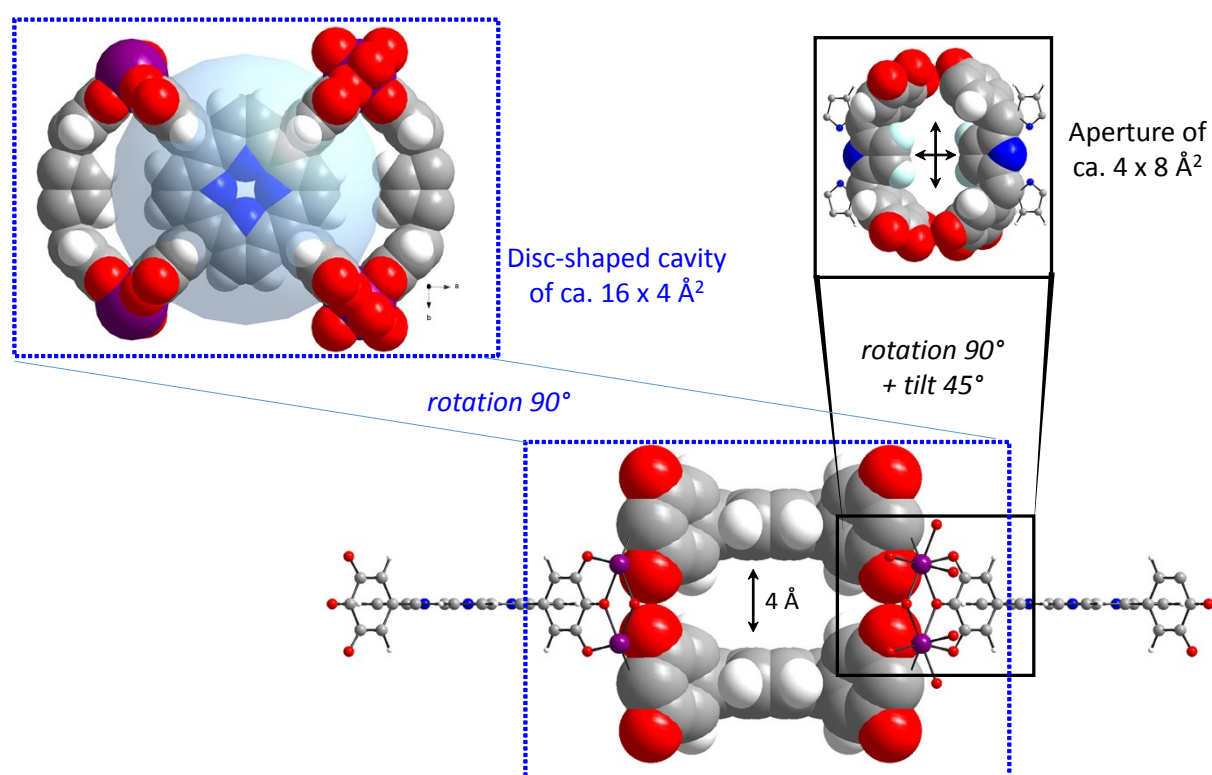


Figure S2. Alternative views of the structure of MIL-173. The disc-shaped pores are highlighted, as well as the pore apertures.

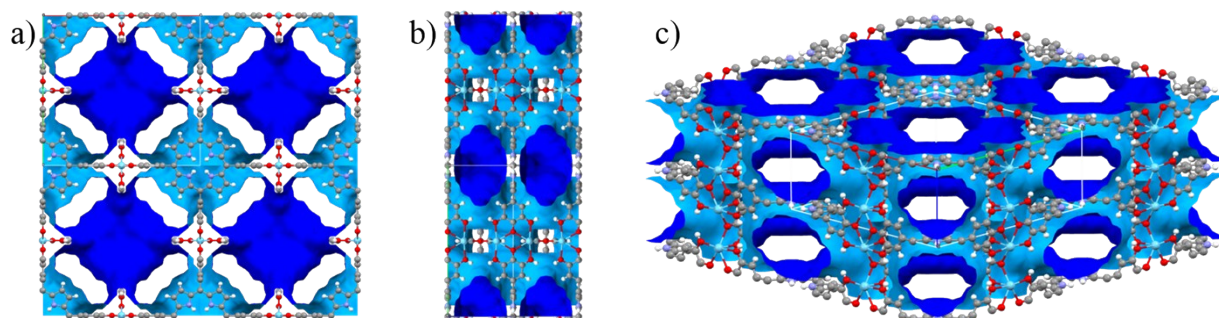


Figure S3. Connolly (or void) surface for MIL-173 generated from the crystalline structure along different axes. The content of the pores has been omitted.

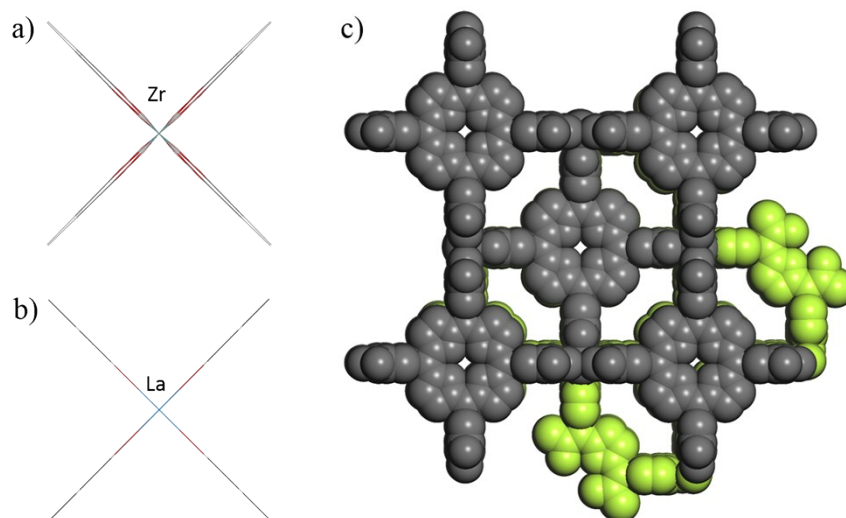


Figure S4. Comparison of the chains M-gallates in a) MIL-173(Zr) and b) MIL-173(La). c) Superposition of the crystalline structures of MIL-173(Zr) (yellow) and MIL-173(La) (grey). H atoms were omitted for the sake of clarity.

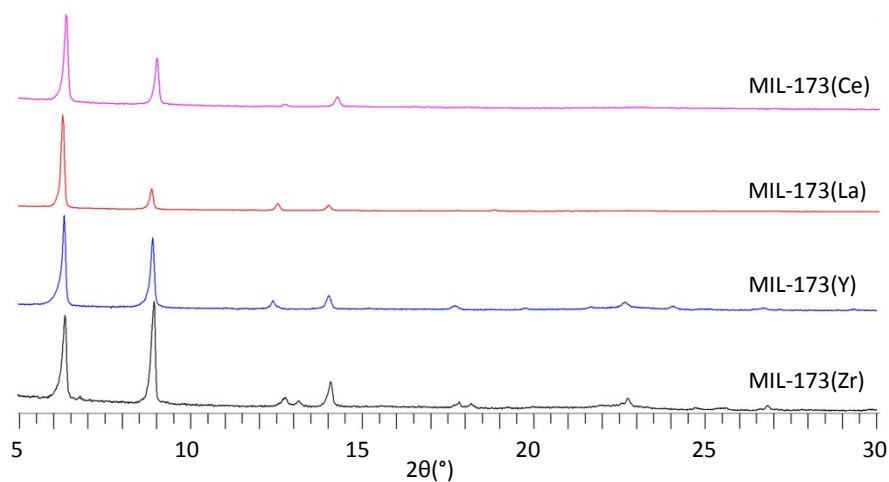


Figure S5. XRPD patterns of MIL-173(La), MIL-173(Ce), MIL-173(Y) and MIL-173(Zr) ($\lambda = 1.5418 \text{ \AA}$).

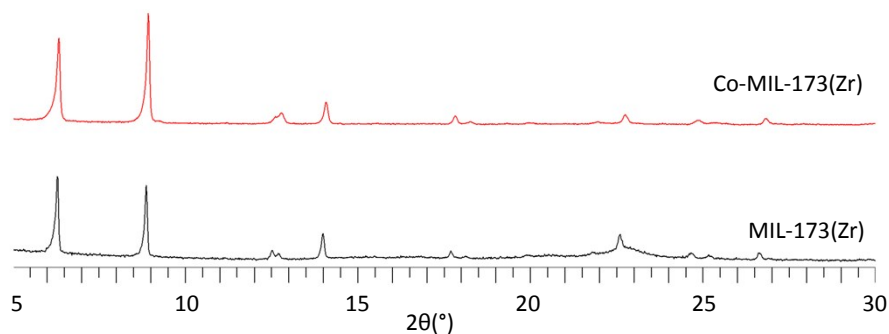


Figure S6. Comparison of the XRPD patterns of Co-MIL-173(Zr) with the one of MIL-173(Zr) ($\lambda = 1.5418 \text{ \AA}$).

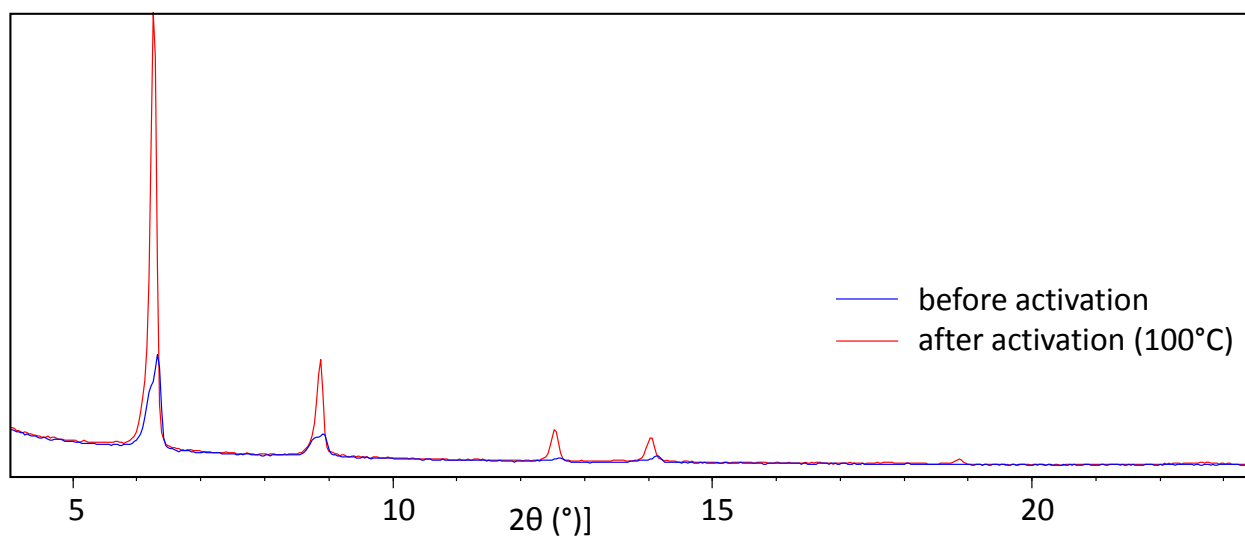


Figure S7. Comparison of the XRPD patterns of MIL-173(La) before (red) and after (blue) activation at 100°C under vacuum for 12 hrs ($\lambda = 1.5418 \text{ \AA}$).

C. SEM and EDX

SEM-EDX analysis was performed on a JEOL JSM-7001F microscope using gold-coated samples equipped with an energy-dispersive X-ray (EDX) spectrometer and a X-Max SDD (Silicon Drift Detector) by Oxford.

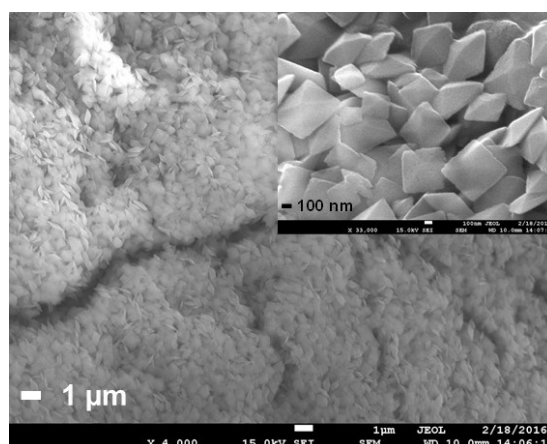


Figure S8. SEM image of MIL-173(Zr) showing the purity and the homogeneity of the sample. Inset shows a zooming on the flattened polyhedral crystals.

Co	37.18	31.65	36.11	30.77	34.05	30.77	41.56	35(4)
Zr	62.82	68.35	63.89	69.23	65.95	69.23	58.44	65(4)

Table S3. Atomic percentage, measured by EDX, after metalation of MIL-173(Zr) with $\text{Co}(\text{OAc})_2$. Raw values are shown, together with the average values (bold).

D. Solid state NMR:

The ^1H and ^{13}C solid-state MAS NMR spectra of all compounds were recorded on an Avance 500 Bruker spectrometer ($B_0 = 11.7$ T), corresponding to Larmor frequencies of 500.1 and 125.7 MHz for ^1H and ^{13}C , respectively. The samples were packed in thin wall 2.5 mm zirconia rotors and spun at 30 kHz. The MIL-173(Y) sample was dried at 100°C prior to the NMR measurement. The ^1H MAS NMR spectra were recorded using a Hahn-echo sequence. The inter-pulse delay was synchronized with one rotor period, the 90° pulse duration was $2.5 \mu\text{s}$, the recycle delay 5 s, and 64 transients were accumulated for each sample. For the $^1\text{H} \rightarrow ^{13}\text{C}$ cross-polarization CPMAS and 2D CP-HETCOR NMR spectra of MIL-173(Zr), 70 and 100 kHz radiofrequency fields were applied on the ^{13}C and ^1H channels, respectively, with a ramped pulse on ^1H . The contact time was 3 ms. ^1H SPINAL-64^[7] decoupling was applied during the ^{13}C signal acquisition. For the 2D spectrum, 66 t_1 slices with 1024 transients each were acquired. The ^1H and ^{13}C chemical shifts are referenced to TMS. The spectra were analysed using the Dmfit^[8] software.

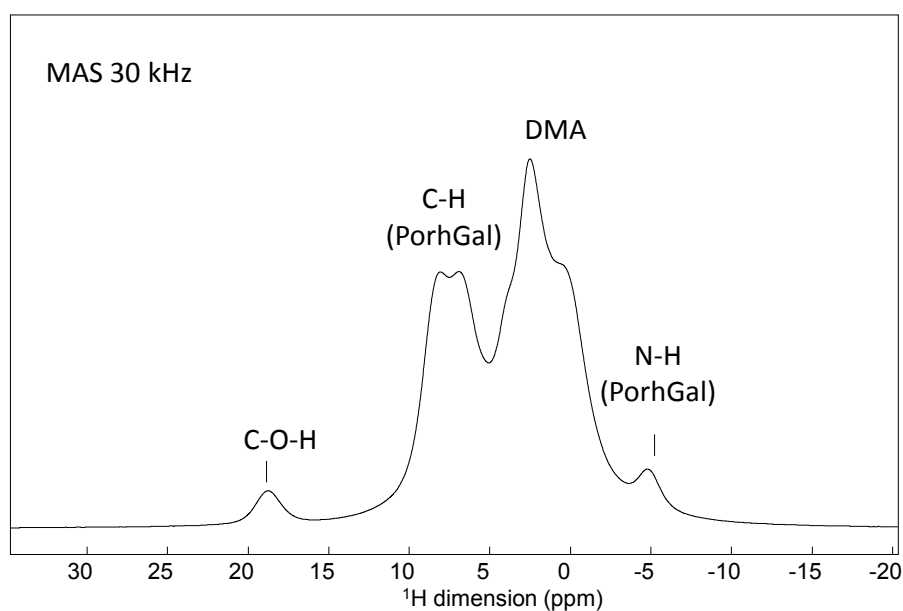


Figure S9. ^1H MAS NMR spectrum of MIL-173(Zr). Note the presence of a very acidic proton at ca 18.5 ppm.

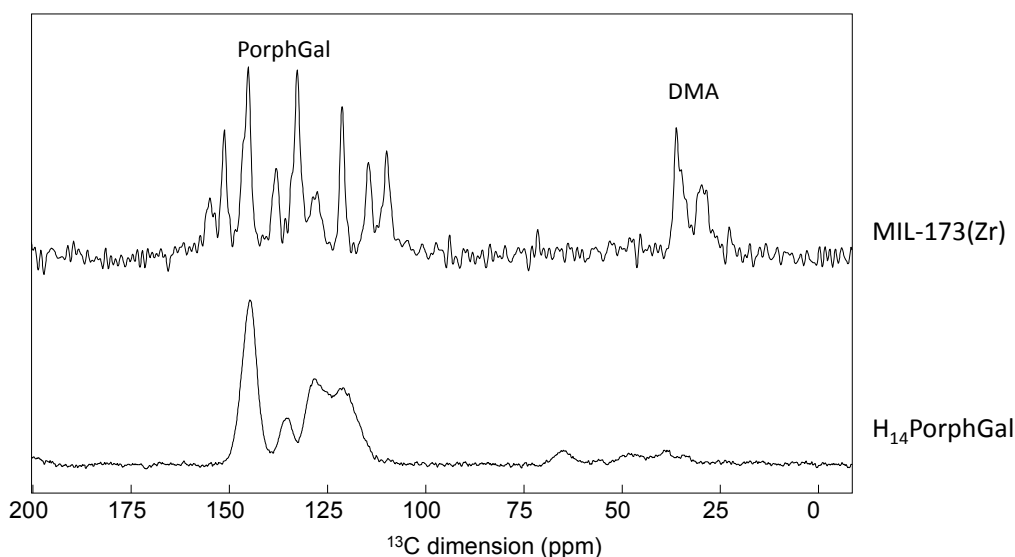


Figure S10. $^1\text{H}\rightarrow^{13}\text{C}$ CPMAS NMR spectrum of MIL-173(Zr) (top) and $\text{H}_{14}\text{PorphGal}$ (bottom). The resonances are partially assigned. This data suggest the absence of DMF (otherwise peaks associated with C=O group would appear at ca. 160 ppm. The existence of multiple peaks in the 25-35 ppm also suggests the presence of at least two crystallographically inequivalent dimethylamine moieties.

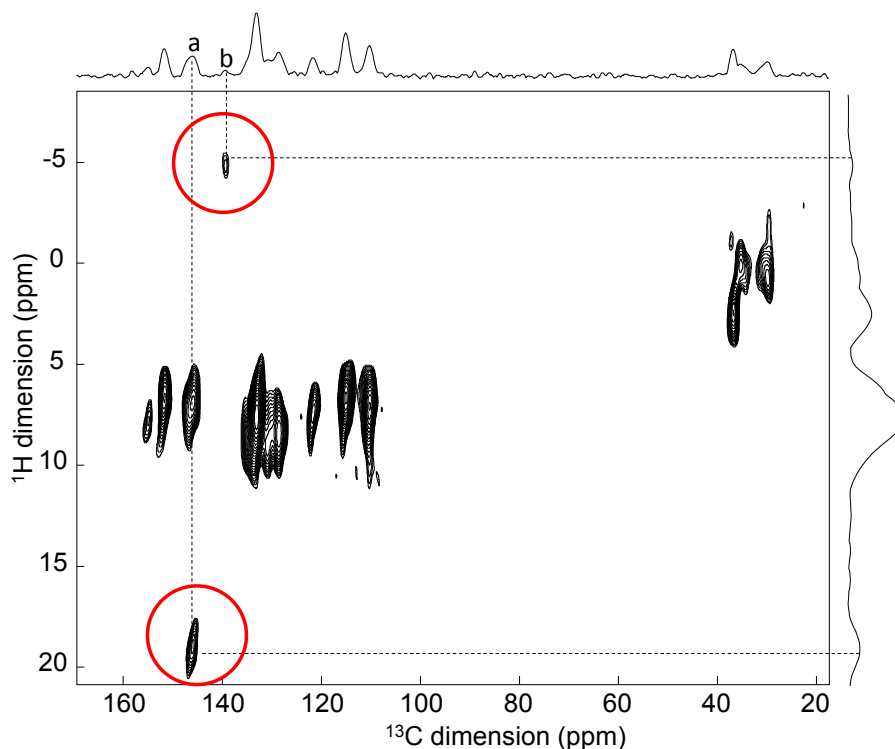


Figure S11. $^1\text{H}\rightarrow^{13}\text{C}$ 2D CP-HECTOR NMR spectrum of MIL-173(Zr). The cross peaks (red circles) indicate the close proximity (i) between the proton at -5 ppm and C-H resonance at 140 ppm, (ii) between the acidic proton (ca. 18 ppm) and the C-O resonance at 145 ppm and hence confirming their attribution to the pyrolic N-H group and C-O(H)-Zr motif respectively. Note

that no cross peak was detected between the acidic proton and the CH₃ resonance at 30-40 ppm, suggesting that is proton is not directly related to a putative dimethylammonium ion.

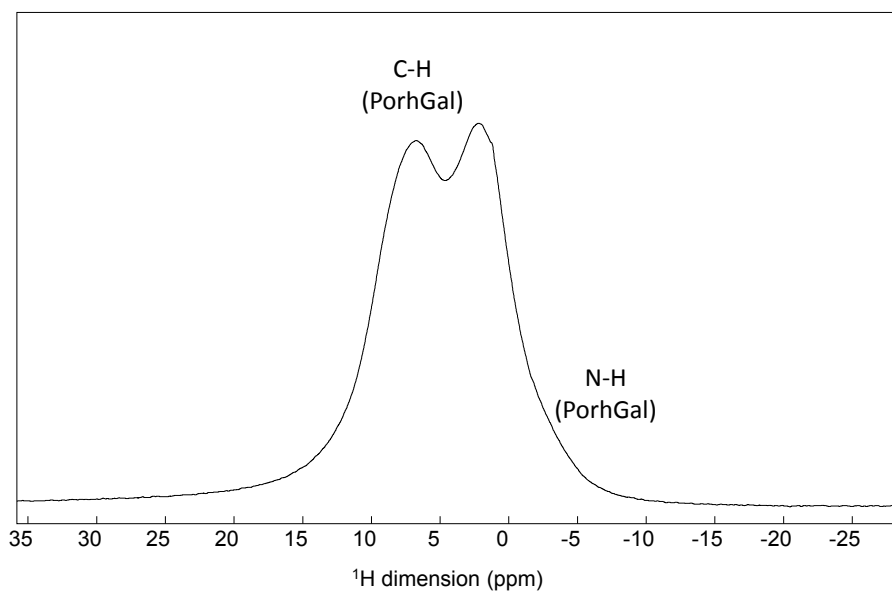


Figure S12. ¹H MAS NMR spectrum of MIL-173(Y). Note the absence of a very acidic proton (>15 ppm).

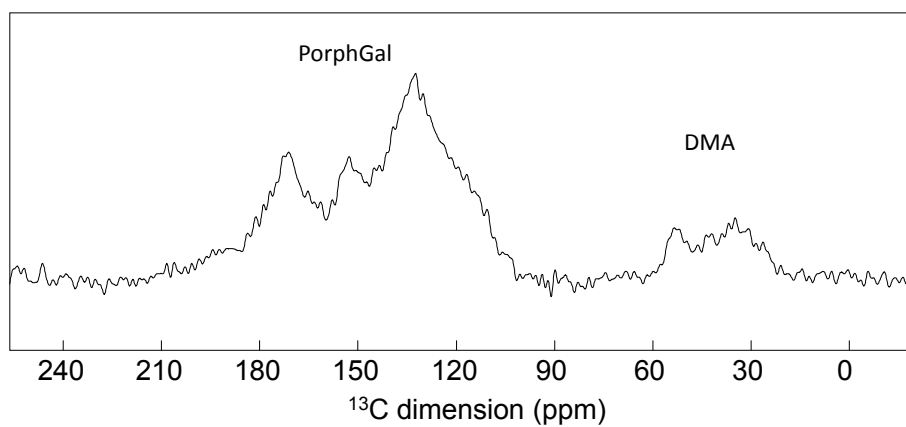


Figure S13. ¹H → ¹³C CPMAS NMR spectrum of MIL-173(Y).

E. N₂ sorption measurements

N₂ sorption measurements were performed at 77 K on BEL Japan Belsorp Mini apparatus. Powder of each solid was previously soaked in methanol during 3 days in order to exchange guest molecules. Then, samples were activated by heating the filtered powder at 100 °C (MIL-173(Zr), MIL-173(Y)) or 120 °C (Co-MIL-173(Y)) under primary vacuum.

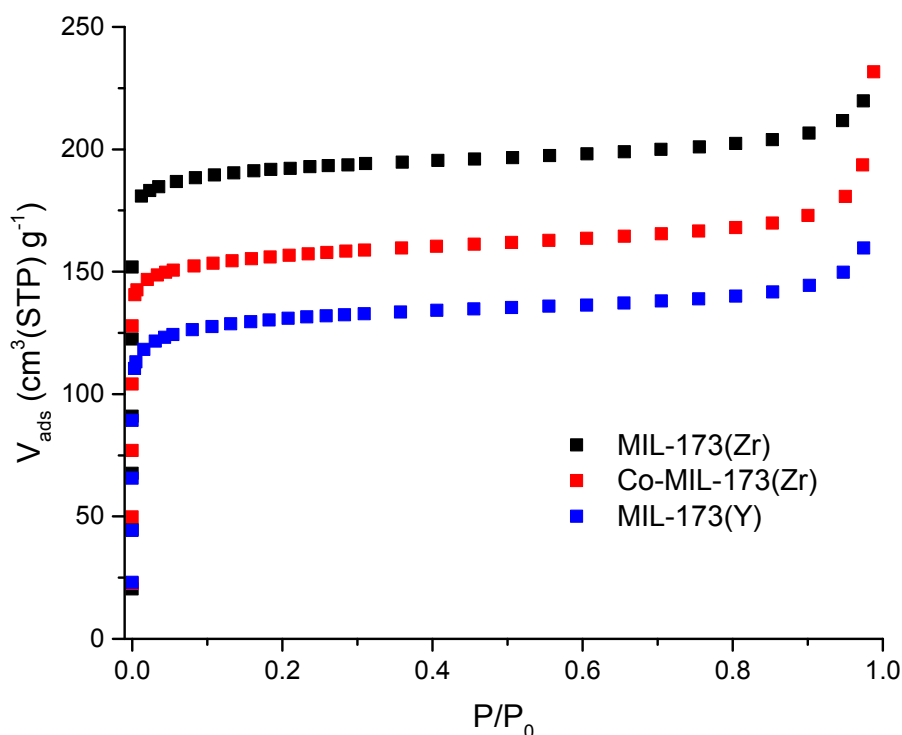


Figure S14. N₂ adsorption isotherms for MIL-173(Y), MIL-173(Zr) and Co-MIL-173(Zr).

F. Thermogravimetric analysis (TGA).

Thermogravimetric analysis (TGA) was performed with a TGA/DSC 1 STARe System from Mettler Toledo. Around 4 mg of sample is heated at a rate of 10 °C·min⁻¹ from 25 to 800 °C, in a 70 μl alumina crucible, under air flow (20 mL·min⁻¹). Data are shown in Figure S15 and deduced mass losses are summarized in Table S4. Note that for MIL-173(RE), the absence of defined plateau precluded any meaningful quantitative analysis.

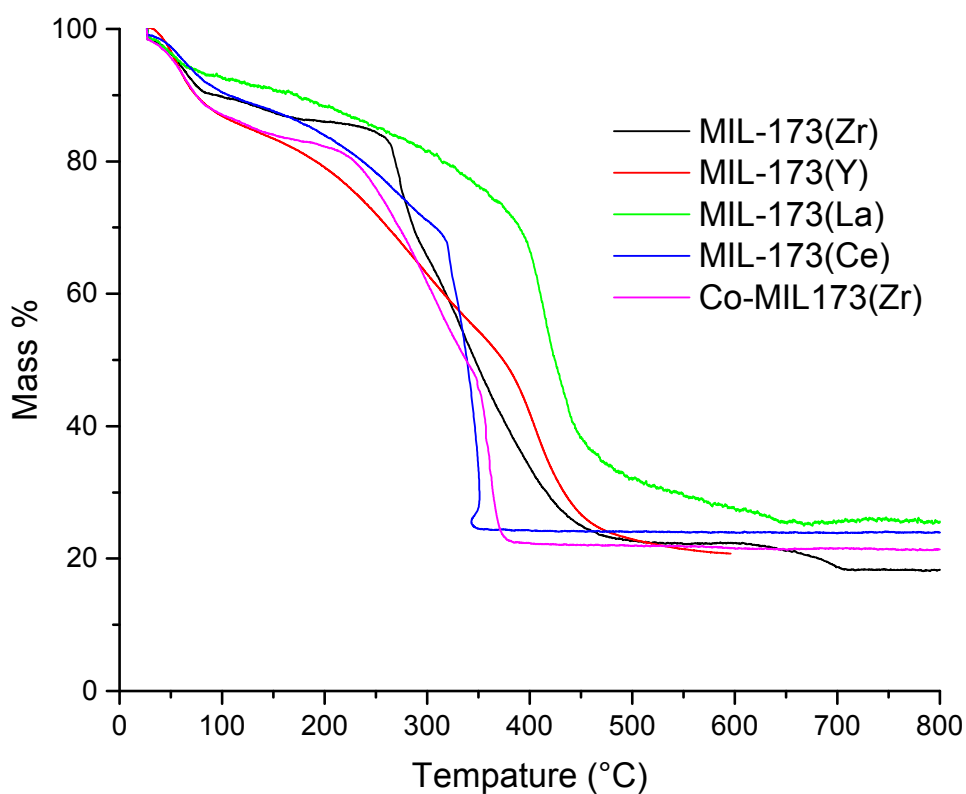


Figure S15. TG curves for MIL-173s.

T(°C)	Proposed formula	Remaining weight (%)	
		Exp.	Calc.
MIL-173(Zr)			
25	$Zr_2(H_6\text{-PorphGal})(DMA)_4(H_2O)_{11}$		
200	$Zr_2(H_6\text{-PorphGal})(DMA)_4$	86	85
800	$2ZrO_2$	18	18
Co-MIL-173(Zr)			
RT	$Zr_2(CoH_4\text{-PorphGal})(DMA)_4(H_2O)_{18}$		
200	$Zr_2(CoH_4\text{-PorphGal})(DMA)_4$	82	79
800	$2ZrO_2 + \frac{1}{2} Co_2O_3$	21	21

Table S4. Experimental and theoretical weight loss for MIL-173(Zr) and Co-MIL-173(Zr).

G. Solid state UV spectroscopy.

Solution state UV spectra were measured on a SAFAS Monaco UV-mc2 spectrophotometer. Solid state UV measurements were performed using a PerkinElmer UV/VIS Lambda 365 spectrophotometer with an integration sphere.

The UV-vis spectra presented in Figure S16 are characteristic of porphyrinic compounds. All the absorption bands originate from π - π^* interactions. Upon metalation, the Soret band (or B band) at ca. 440 nm is slightly shifted (from 435 in MIL-173(Zr) to 444 nm in Co-MIL-173(Zr)), while the number of Q bands (above 500 nm) is reduced. This is agreement with what is commonly observed upon metalation of porphyrins,^[9] and further confirm the absence of remaining free porphyrin base in the metalated solid.

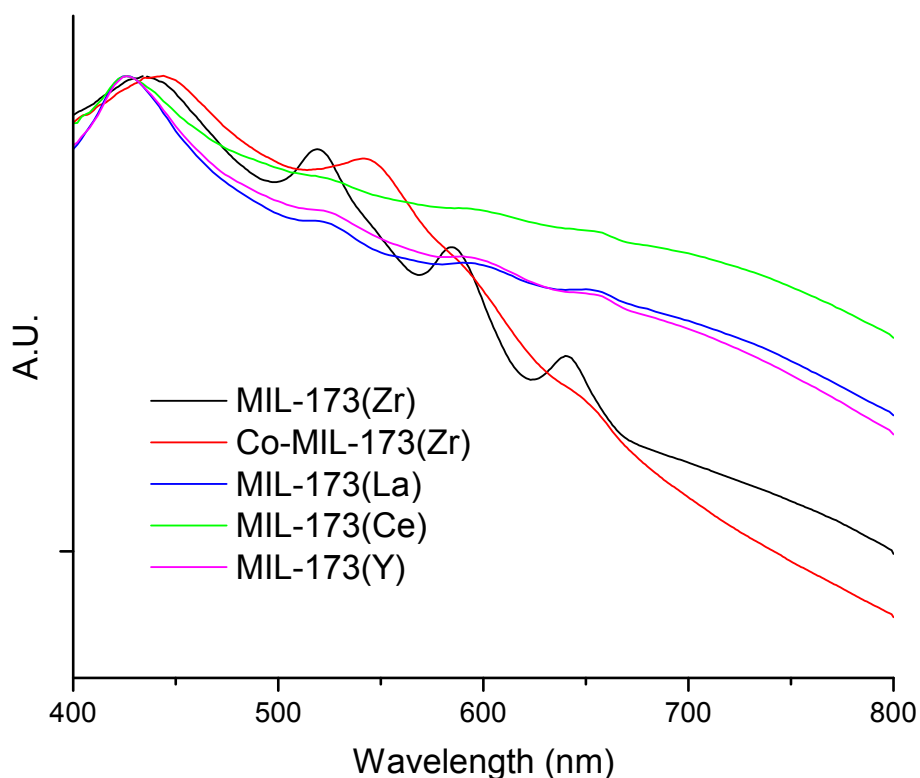


Figure S16. Comparison of the normalized solid state UV-visible absorption spectra of MIL-173(Zr) before (black) and after (red) metalation with cobalt(II) acetate. Data are also shown for the non metalated MIL-173(RE) (RE = La, Ce, Y).

H. Stability tests

20 mg of the solids (MIL-173(Zr), Co-MIL-173(Zr), MIL-173(Y)) were suspended for one week in 20 mL of either water or a phosphate buffer saline solution (PBS; 0.01 M, pH = 7.4) in a closed vial at 37°C (130 rpm; incubator Multitron Orbitale 50mm, HT Infors, France). The solids were then recovered by centrifugation, washed 3 times with water, once with EtOH, and finally dried in air.

I. EPR measurements

EPR spectra were acquired using a Bruker EMX instrument operating at X-band frequency. Co-MIL-173(Zr) (20 mg) was activated at 80 °C under vacuum for 3 h. The EPR spectrum of the solid was recorded at 100 K. Then, the sample was exposed to oxygen using a balloon and the EPR spectrum recorded again at 100 K.

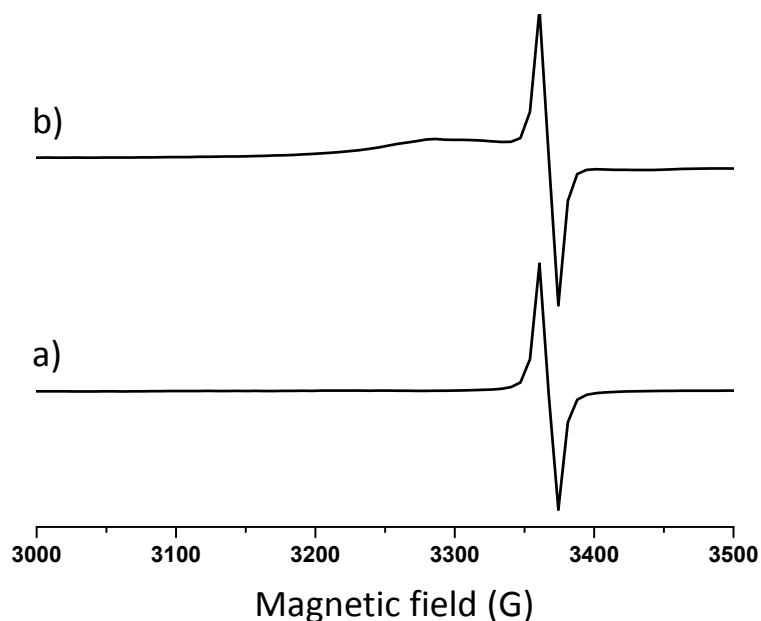


Figure S17. EPR spectra of Co-MIL-173(Zr) after activation at 80°C under vacuum for 3 h in the absence (a) and in the presence (b) of O₂. Data were recorded at 100 K.

J. Raman experiments

Raman spectra of Co-MIL-173(Zr) solid were recorded on a Renishaw Raman Spectrometer (“Refelx”) with a 514 nm laser excitation (25 mW) equipped with a CCD detector. A commercial Linkam cell (THMS600) was used for collecting spectra under controlled conditions. Briefly, the sample was first subjected to a N₂ flow (20 mL min⁻¹) at 120 °C for 3 h. Subsequently, the gas was changed to O₂ (20 mL·min⁻¹) at the same temperature. Afterwards, the temperature was lowered to 20 °C in O₂ flow and changed to N₂. Finally, spectra were collected after sample exposure at 20 °C under N₂ flow.

K. Catalytic tests

Chemicals. All the reagents and solvents employed for catalytic experiments (i.e. indane, cumene, 1,3-diisopropylbenzene) were of analytical or HPLC grade and supplied by Sigma-Aldrich. The benzylic substrates were distilled before use to remove radical quenchers.

Catalytic experiments. 2 mg of Co-MIL-173(Zr) or MIL-173(Zr) (~1.7 μmol) were added to a round-bottom flask (25 mL). Catalyst activation was carried out overnight at 120 °C under vacuum. The reaction system was purged with molecular oxygen using a balloon, then the substrate was introduced (20 mmol) and the system was sonicated for 5 min. Then, reaction mixture was placed in a pre-heated bath at 120 °C and magnetically stirred. Reusability of Co-MIL-173(Zr) was performed under the same reaction conditions. At the end of the reaction, the catalyst was filtered through a Nylon membrane filter of 0.2 μm . Then, the solid was placed in a round-bottom flask containing methanol and the system heated at 60 °C for 2 h. This washing procedure was repeated two more times. Then, the catalyst was dried at 100 °C for 18 h and used in a second catalytic cycle.

Product analysis. Previously filtered reaction aliquots (100 μL) were diluted in a toluene solution (500 μL) containing a known amount of nitrobenzene as the external standard. Then, the reaction aliquots were analyzed by gas chromatography using a flame ionization detector. Quantification was carried out by using calibration curves of authentic samples. Benzylic hydroperoxides were quantified by reacting the sample aliquots with triphenylphosphine and, thus, the phosphine oxide allowed quantification.

Leaching measurements. At the end of the reaction the reaction mixture still hot was removed by filtration. Then, the organic phase was stirred with concentrated nitric aqueous solution (HNO_3 , 3 M) and the system heated at 80 °C for 24 h to extract the metal ions. The metal content of the aqueous phase was analyzed by chemical analysis using an ICP-AES instrument.

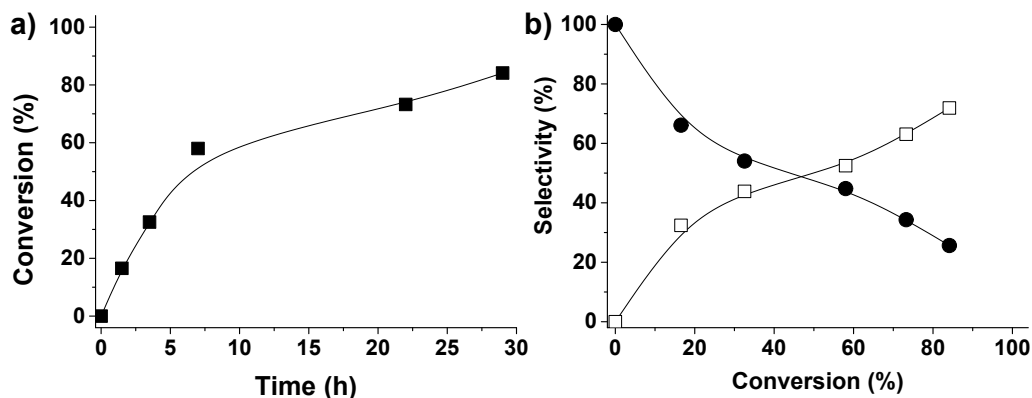


Figure S18. Time conversion plot (a) and conversion-selectivity plot (b) for the aerobic oxidation of cumene using Co-MIL-173(Zr) as catalyst. Legend panel b: cumyl hydroperoxide (●) and cumyl alcohol (□).

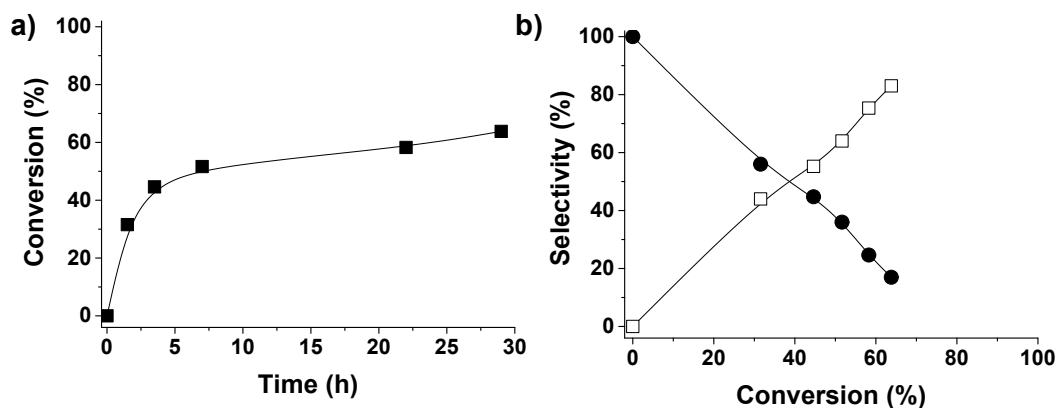


Figure S19. Time conversion plot (a) and conversion-selectivity plot (b) for the aerobic oxidation of 1,3-diisopropylbenzene using Co-MIL-173(Zr) as catalyst. Legend panel b: mono hydroperoxide of 1,3-diisopropylbenzene (●) and mono alcohol of 1,3-diisopropylbenzene (□).

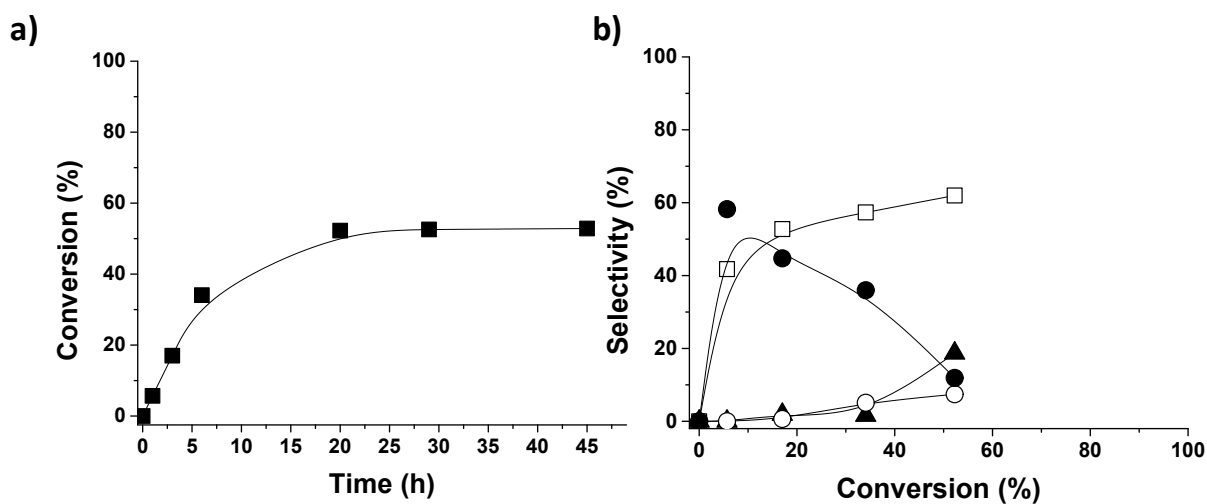


Figure S20. Time conversion plot (a) and conversion-selectivity plot (b) for the aerobic oxidation of 1,3,5-triisopropylbenzene using Co-MIL-173(Zr) as catalyst. Legend panel b: mono hydroperoxide of 1,3,5-triisopropylbenzene (●), mono alcohol of 1,3,5-triisopropylbenzene (□) di alcohol of 1,3,5-triisopropylbenzene (○) and alcohol and ketone of 1,3,5-triisopropylbenzene (▲).

References

- [1] L. Jiang, F. Lu, H. Li, Q. Chang, Y. Li, H. Liu, S. Wang, Y. Song, G. Cui, N. Wang, et al., *J. Phys. Chem. B* **2005**, *109*, 6311–6315.
- [2] *Topas V5: General Profile and Structure Analysis Software for Powder Diffraction Data*, Bruker AXS Ltd, **2014**.
- [3] A. Altomare, M. C. Burla, M. Camalli, B. Carrozzini, G. L. Casciarano, C. Giacovazzo, A. Guagliardi, A. G. G. Moliterni, G. Polidori, R. Rizzi, *J Appl Crystallogr* **1999**, *32*, 339.
- [4] *CrysAlisPro*, Oxford Diffraction Ltd., **2010**.
- [5] G. M. Sheldrick, *Acta Crystallogr. Sect. C Struct. Chem.* **2015**, *71*, 3–8.
- [6] A. L. Spek, *Acta Crystallogr. Sect. C Struct. Chem.* **2015**, *71*, 9–18.
- [7] B. M. Fung, A. K. Khitrin, K. Ermolaev, *J. Magn. Reson.* **2000**, *142*, 97.
- [8] D. Massiot, F. Fayon, M. Capron, I. King, S. Le Calvé, B. Alonso, J. O. Durand, B. Bujoli, Z. Gan, G. Hoatson, *Magn. Reson. Chem.* **2002**, *40*, 70.
- [9] *The Porphyrin Handbook*, K. M. Kadish, K. M. Smith, R. Guilard, **2000**.